Microwave ablation antenna for functional adenomas in the adrenal gland

Microwave ablation antenna for functional adenomas in the Adrenal Gland

L. Farina[1,2], **A. J. de Marco**[3,4], **A. Bottiglieri**[1], **G. Ruvio**[1,5], **J. Eaton-Evans**[1,5], **M. C. Dennedy**[6], **M. E. Adnan**[1], **and M. OHalloran**[1]

[1]Translational Medical Device Lab, National University of Ireland Galway, Galway, Ireland
[2]CÚRAM, National University of Ireland Galway, Galway
[3]Department of Physics, University of Malta, Msida, Malta
[4]Department of Aeronautics, Imperial College London, London, UK
[5]Endowave Ltd., Ireland
[6]Department of Pharmacology and Therapeutics, National University of Ireland Galway, Galway, Ireland

Abstract— Microwave thermal ablation has been thoroughly investigated in the last decades. However, new challenges for this technology are nowadays represented by specific applications. The present work investigates a promising ablative solution for the treatment of functional adenomas in the adrenal gland. A numerical study conducted to build and test an optimized internally cooled triaxial antenna will be presented. The antenna has been designed to minimize its transversal dimension merging radiating and cooling elements. The proposed antenna has been then built in our laboratories and experimentally tested on *Ex vivo* biological tissues. Numerical and experimental results will be reported and discussed.

1. INTRODUCTION

Microwave thermal ablation (MWA) is a widespread minimally–invasive technique used for the treatment of different solid tumors [1]. MWA exploits the interaction between the electromagnetic (EM) field radiated by an antenna at microwave frequencies and the target biological tissue to induce a cytotoxic temperature increase [1]. The technique is nowadays well investigated and the researchers in the field focus their work in the development of accurate treatment planning and tools for the physicians [2]. Lately, the application of MWA to specific and novel targets and areas has been considered [3]. In this scenario, microwave thermal ablation has been recently taken in consideration for the treatment of medical conditions correlated or caused by anomalies in the adrenal gland.

Functional adenomas in the adrenal gland are the cause of sever hypertensive clinical conditions. The most common form of secondary hypertension is represented by Primary aldosteronism (PA) (or Conns syndrome). Primary Aldosteronism (PA) represents up to 12 % of all cases of hypertension within the population [4] - [6]. In patient with resistant hypertension, the prevalence of PA approaches 20 % [6]. The most commonly performed treatment for PA is adrenalectomy: the complete removal of the adrenal gland. Unfortunately, PA often reoccurs in the remaining contralateral adrenal gland. In such cases, and in the case of bilateral diseases (60 % of the cases) [6], the patient is managed with pharmaceuticals which are poorly tolerated due to their side effects. Thermal ablation treatments have been primary used to remove the entire adrenal gland (i.e. thermal adrenalectomy) showing detrimental effect [7], but lately they have been proposed to locally eliminate adenomas in the adrenal gland [8]. MWA has been mainly adopted to eliminate adrenal metastasis due to its ability to induce larger lesions; but its safety and efficacy have been investigated also in the treatment of functional adenomas [9] - [11]. The advantage linked to MWA is the ability to efficaciously and safely treat small target, as well as large lesion. Moreover, MWA does not require long treatment time (less than 20 min), that not only reduces the whole time of the intervention, with obvious effects on time-cost efficacy and patient-stress, but it reduces the time of stimulation of the adrenal gland and the subsequent occurrence of hypertensive crisis [11].

Microwave ablation represents a valuable solution to locally eliminate adenomas preserving the healthy functional adrenal tissue surrounding the adenoma and proximal sensitive structures (e.g. blood vessels, nerves). The benign shallow hormone-eluding adenomas are usually small and located in the gland cortex periphery. The adrenal cortex protects the medulla, that regulates the blood pressure through the adrenaline production, and it is surrounded by a fat of layer with embedded arteries. A well-focused and controlled ablation is required to selectively treat these

adenomas, sparing the healthy adrenal tissue and the surrounding sensitive structures such as nerves or blood vessels. Since puncturing of the gland is undesirable, the optimal positioning of the ablation antenna would be parallel to the adenoma at the interface between the gland and the fat layer. Additionally, the applicator would be required to be directional and operate only in a preferred direction. To reach this objective, several study in the literature have presented directive applicators [12] - [14]. The drawbacks of this proposed solution are mainly two. First, the increase of the transversal dimension of the antenna and thus the increase of its invasiveness: in a target as small as the adrenal gland (about 15 cm^3 [15]) an increase of even less than 1 mm in diameter can be noticeable. Second, directive antennas must be precisely oriented accordingly with the preferred direction: this requirement represents a complication of the clinical procedure and discourages clinicians from adopting this solution in the treatment of functional adenomas of the adrenal gland. Other studies have suggested the exploitation of the natural presence of the fat layer surrounding the adrenal gland to obtain directive pattern of ablation [15] -[17]. These studies illustrated how the interface between two tissue with high contrast in dielectric properties (e.g. fat/adrenal cortex, or fat/muscle) can affect the radiation pattern of a simple monopole omnidirectional antenna to obtain an ablation in a preferred direction.

Due to the elevate heterogeneity and reduced dimensions of the target area (adrenal gland), the ablative performances of the antenna can vary in correlation with the antenna detuning. To overcome this issue, in this study, we present a triaxial structure obtained starting from a monopole antenna equipped with a cooling system based on polyimide tubes and replacing the inner tube of the cooling system with a stainless-steel tube. The distance of this tube from the feed point of the monopole antenna was tuned to optimize the electromagnetic energy transfer without reducing the flux cooling water efficiency. The proposed antenna, operating at 2.45 GHZ, guarantees minimal–invasiveness (16–gauge) and robustness, allowing the clinicians to operate in optimal conditions independently from the antenna insertion depth and orientation.

The paper is organized as follows. In Section 2, we present the numerical and experimental methodology, providing the details about the antenna designing and prototyping. The adrenal gland model presented in [15] is exploited to perform numerical studies. The prototyped antenna is experimentally tested in *ex vivo* liver and muscle. Next, in Section 3, the numerical and *ex vivo* experimental results in terms of antenna performance improvement and ablation shape induced are presented and discussed.

2. METHODOLOGY

2.1. Numerical study

A 3D commercial full–wave electromagnetic software (CST MWS Suite 2018, Darmstadt, Germany) was adopted to conduct the numerical study. First the MWA applicator was modelled as a simple 23–gauge monopole antenna with the characteristics of an UT–020 coaxial cable Table 1. A parametric study for different monopole tip lengths, i.e. from 12.0 mm to 4.0 mm, was conducted. The optimal length of the exposed tip was selected to obtain the minimum reflected power and the maximum resonance bandwidth of the reflection coefficient (S_{11}) at the operating frequency of 2.45. Then, the optimized monopole antenna was inserted in a third concentric 18-gauge stainless-steel tube; the optimal distance of the end of this third tube from the antenna feed point was investigated through a parametric simulation. The parametric sweep was conducted varying the positioning of the stainless-steel tube with respect to the base of the monopole tip from -5.5 mm to 2.5 mm. The reflection coefficient for the different proposed configurations was tested in water. Finally, an external 16–gauge polyimide tube was used to complete the flowing paths of the integrated cooling system. The stainless-steel tube provides the onward path of water flow, whereas the outer polyimide tube provides the return flow path.

The performances of the two designed ablation applicators, equipped with the refrigerating system, were tested in liver in terms of the magnitude of the reflection coefficient and in terms of the resonance bandwidth within the 0–3 GHz frequency range. The antennas were placed at the center of a block mimicking the mechanical, electric and thermal properties of the chosen biological tissue. Two different antennas insertion depth (10 and 30 mm from the feed point) were also tested to verify the improved robustness of the triaxial antenna with respect to the coaxial one. Finally, the triaxial antenna was placed in the adrenal numerical model presented in [15], parallel to the interface between adrenal cortex and fat. The dielectric properties of liver and fat, as well the values related to heat capacity, thermal conductivity and density were manually loaded in the material settings of the CST MWS software from the ITIS database (ITIS Foundation, Zurich, CH). The

Inner Conductor Diameter	0.127 mm
Inner Conductor Material	Copper (Annealed)
Dielectric Outer Diameter	0.419 mm
Dielectric Material	PTFE
Outer Conductor Outer Diameter	0.584 mm
Outer Conductor Material	Copper (Annealed)

Table 1: UT-020 coaxial cable characteristics.

thermal properties of the adrenal gland were obtained from the same source, while the dielectric properties were obtained from [18]. A tetrahedrons-based meshing, denser for the material with higher relative permittivity, was used. The water temperature of the cooling system was fixed at 18 °C during all simulations. Due to the *ex vivo* experimental scenario proposed, the starting temperature was considered at 25 °C for the biological tissues and the blood perfusion parameters were not included. Coupled electromagnetic (EM) and thermal simulations were executed for a single power level of 60 W for a treatment duration of 60 s.

2.2. Experimental study

The designed triaxial antenna was prototyped in our laboratory. A monopole antenna with an exposed tip of 6.5 mm was made with a UT-020 coaxial cable (Micro–Coax Inc., Pottstown, PA, US); it was inserted in an 18-gauge stainless-steel tube, positioned 0.5 mm away from the monopole base, and in a 16-gauge polyimide casing to implement efficient water cooling. The stainless-steel tube was simultaneously used for the antenna cooling system and to improve the antenna performance. A SMA connector was placed at 165.0 mm from the antenna feed-point. The fabricated antennas performances were evaluated in terms of reflection coefficient (S_{11}) by connecting the antenna to an antenna analyser (Rohde & Schwarz® ZVH8 100 kHz - 8 GHz) through a low–phase coaxial cable. A full one–port calibration procedure was performed, considering three different calibration standards: open circuit, short circuit and 50 Ω load. Measurements were conducted in water at room temperature. The S_{11} values were recorded at 201 linearly spaced frequency points over 0 - 3 GHz.

The in–house triaxial antenna was then used to conduct *ex vivo* experimental studies to test its performances. The experiments were conducted on *ex vivo* lamb liver and porcine muscle. The temperature of the material under test was measured using an infrared thermometer (Fluxe 62 Max IR Thermometer, -30°C – 500°C temperature range, accuracy of 1.5 °C of reading at temperature $\geq$ 0 °C). A single power level of 60 W was set at the microwave generator (Sairem, SAS, France) at 2.45 GHz. Ablations were performed for 30, 60 and 90 s in liver, and for 60 s in muscle, for a total of 6 experiments. A peristaltic dispensing pump (DP2000, Thermo-Fisher Scientific Inc., Waltham, Massachusetts, US) was connected to the inflow channel of the ablation applicator, operating at 50 ml/min. After each experiment, radial and longitudinal ablation extents were measured by a millimeter ruler. The longitudinal dimension was evaluated parallel to the antenna axis and the radial dimension was measured perpendicularly to the antenna axis at the feed-point.

3. RESULTS

3.1. Numerical study

The MWA antenna performances were evaluated in terms of the magnitude of the reflection coefficient and in terms of the resonance bandwidth within the 0–3 GHz frequency range. From the parametric simulations conducted in water, the optimal tip length of the MWA 23–gauge monopole antenna was found to be 6.5 mm; whereas the optimal distance of the third concentric 18–gauge stainless-steel tube from the feed point resulted -0.5 mm. The performances of the optimized monopole and triaxial antennas were tested in liver for two different insertion depth: 10 and 30 mm from the feed point. The reflection coefficients (S_{11}) simulated are reported and compared in Figure 1: it is possible to observe that the third metallic element guarantees the antenna matching independently from the antenna insertion depth, ensuring less than 10% of reflected power.

The triaxial antenna was adopted to conduct coupled EM-thermal simulation to investigate the effect of the target area heterogeneity on the resulting ablation zone. A single setting of 60 W – 60 s was tested placing the antenna in liver and in an adrenal numerical model [15]. The adrenal model is proposed as generic representative of an heterogeneous scenario. A simulated reflection coefficients (S_{11}) of -10 dB is guaranteed also in the adrenal gland model. Figure 2 illustrates

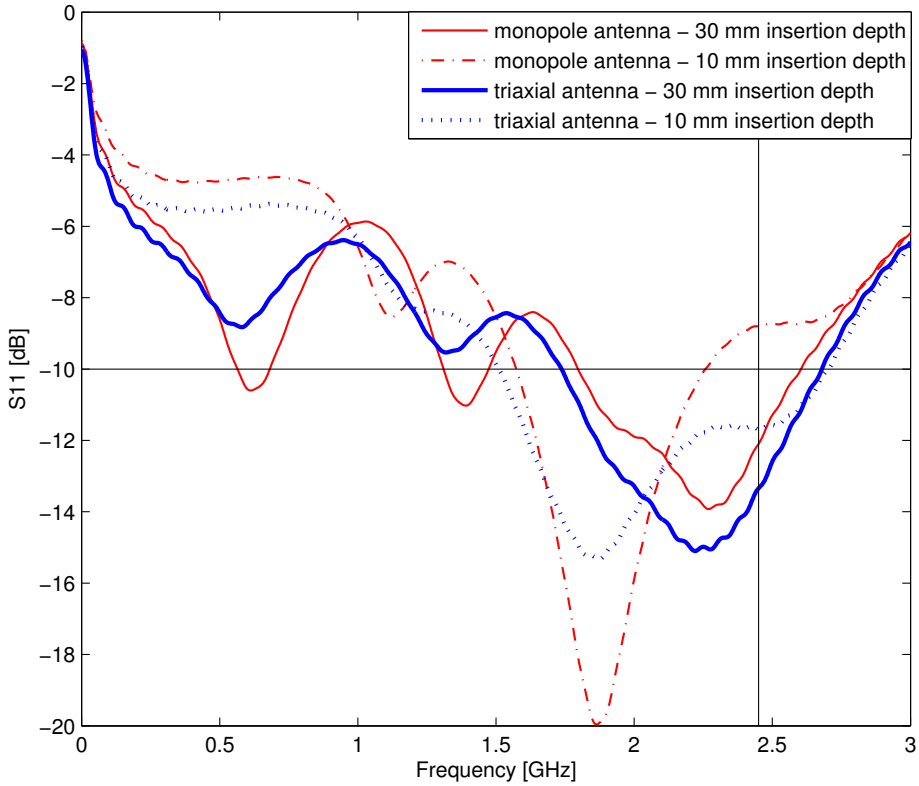

Figure 1: Simulated antenna reflection coefficient (S_{11}) over the 0-3 GHz range in liver. The S_{11} of the monopole and triaxial antennas are reported for the two tested antenna insertion depths. The insertion depth is calculated as distance from the antenna feed. The frequency point of interest is highlighted (2.45 GHz); as well as the -10 dB level required to guarantee a satisfying antenna match and corresponding to the 10 % of reflected power.

the thermal profiles obtained from the simulations. The edge of the thermally ablated region is considered where the tissue reaches a temperature of approximately 55–60 °C [19], thus in the figure, the estimated ablation zone is represented by the red area. Figure 2 confirms a possible shielding effect of a tissue with low dielectric properties, resulting in a directive ablation pattern, as desired, independently from the antenna orientation [16],[17], for controlled settings of power and time.

3.2. Experimental study

The triaxial MWA antenna used in the experimental study showed a reflection coefficient of -18 dB at the operating frequency 2.45 GHz. This value resulted as an improvement of the reflection coefficient measured for the monopole antenna (-14 dB) before adding the stainless-steel tube, during the antenna fabrication.

The final antenna prototype was used to conduct different *ex vivo* tests (N=6). In liver, a 3 % of reflected power was observed for all the experiments, whereas in muscle, a 7 % of reflected power was observed. Table 2 summarizes the experimental settings and the results obtained; while Figure 3 illustrates the ablation areas experimentally obtained with the different settings. It is possible to observe that the results obtained in the simulation are confirmed by the experimental practice. A good sphericity in the ablation zones obtained in liver for 60 and 90 s is noticeable (≥ 0.85), while for shorter time of ablation a poor sphericity is observed.The ablation zone in muscle results 30 % bigger than in liver, given the same power and time settings, and a sufficient sphericity index is guaranteed (> 0.75). A structural difference in the two tissue (i.e. the directionality of the muscle fibres) and a difference in the dielectric properties can determine a different absorption of the EM field [20].

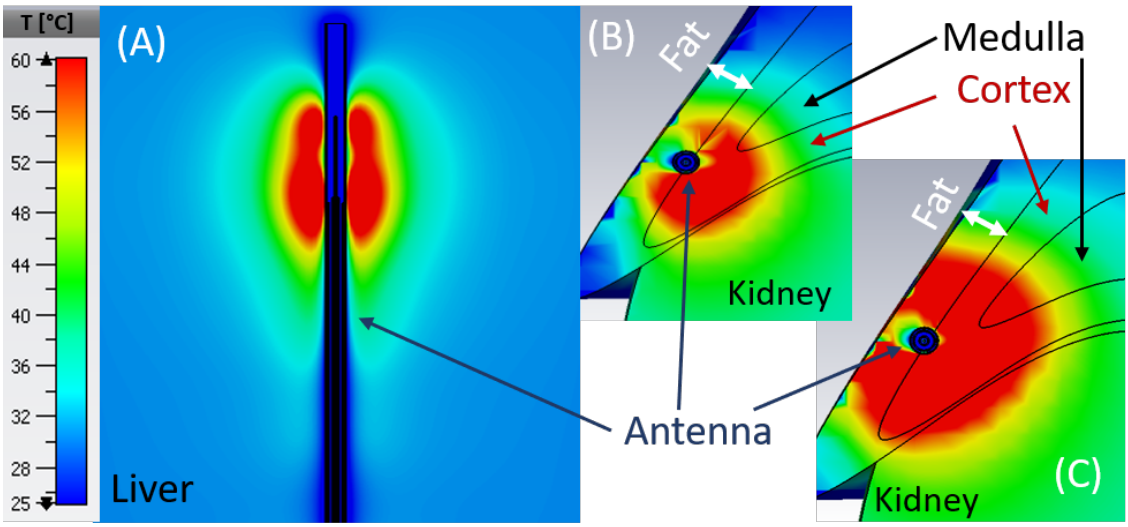

Figure 2: Simulated temperature patterns obtained with the triaxial antenna operating at 60 W for 60 s, in liver (A) and in the adrenal gland model (B, C), accounting for medulla, cortex, kidney and fat. (B) is the thermal profile after 30 s of ablation and (C) at the end of the 60 s of ablation. The red represent temperature $\geq$ 60 °C, i.e. the estimated area of ablation.

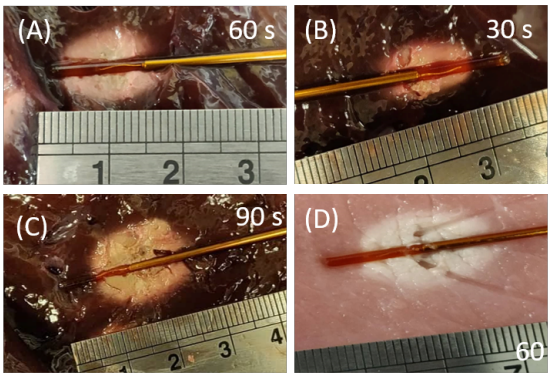

Figure 3: Experimental ablation zones in lamb liver (A, B, C) and in porcine muscle (D). The in-house triaxial antenna is illustrated in place. All the ablation has been conducted at 60 W for 60 s (A, D), 30 s (B) and 90 s (C).

Tissue	**N**	**Power [W]**	**Time [s]**	**Radial d. [mm]**	**Longitudinal d. [mm]**	**Sphericity**
Liver	3	60	60	10	12	0.85
Liver	1	60	30	6	10	0.6
Liver	1	60	90	14	16	0.875
Muscle	1	60	60	13	17	0.765

d.= dimension

Table 2: Experimental results summary.

4. CONCLUSION

In this work, an optimized minimally–invasive triaxial antenna are presented, designed and prototyped. The performance improvements linked to the introduction of a third metallic element to a monopole antenna are numerically illustrated. The triaxial antenna introduces robustness to the antenna performances, guaranteeing a good impedance matching even for reduced insertion depth (10 mm). The prototyped antenna was successfully tested in *ex vivo* biological tissues.

Exploiting the stainless-steel tube as element of the cooling system, the antenna radial dimension is not enlarged and the cooling efficacy is preserved. The possibility of using the proposed antenna in heterogeneous scenario has been numerically proved. This ablative solution would permit the clinicians to efficiently and safely use an ablation device for the treatment of functional adenomas of the adrenal gland, without caring of the antenna orientation and insertion depth. Further study should be conducted to validate the proposed antenna and its application in adrenal gland models *ex vivo* and *in vivo*.

ACKNOWLEDGMENT

The research leading to these results has received funding from the European Research Council under the European Unions Horizon 2020 Programme (H2020)/ERC grant agreement n.637780 and ERC PoC Grant REALTA n.754308. This project has received funding from the European Unions Horizon 2020 research and innovation programme under the Marie Skodowska-Curie grant agreement No 713690.

REFERENCES

1. M. Ahmed, et al., "Principles of and advances in percutaneous ablation," *Radiology*, Vol. 258, No. 2, 351–369, 2011.
2. V. Lopresto, et al., "Microwave thermal ablation: effects of tissue properties variations on predictive models for treatment planning," *Med Eng Phys* , Vol. 46, 63–70, 2017.
3. P. Liang, et al., *'Microwave Ablation Treatment of Solid Tumors*, Springer, Dordrecht, 2015.
4. P. Mulatero, et al., "Increased Diagnosis of Primary Aldosteronism, Including Surgically Correctable Forms, in Centers from Five Continents," *J Clin Endocrinol Metab* , Vol. 89, No. 3, 1045–1050, 2004.
5. G. P. Rossi, et al., "A Prospective Study of the Prevalence of Primary Aldosteronism in 1,125 Hypertensive Patients," *JACC* , Vol. 48, No. 11, 2293–2300, 2006.
6. W. F. Jr Young, "Adrenal causes of hypertension: Pheochromocytoma and primary aldosteronism," *Rev Endocr Metab Disord* , Vol. 8, 309–320, 2007.
7. k. Yamakodo, et al., "Adrenal Radiofrequency Ablation in Swine: Change in Blood Pressure and Histopathologic Analysis," *Cardiovasc Intervent Radiol* , Vol. 34, 839–844, 2011.
8. A. Aronova, et al., "Management of hypertension in primary aldosteronism," *World J Cardiol* , Vol. 6, No. 5, 227–233, 2014.
9. Y. Wang, et al., "Ultrasound-guided percutaneous microwave ablation of adrenal metastasis: Preliminary results," *Int. J. Hyperthermia* , Vol. 25, No. 6, 455–461, 2009.
10. F. J. Wolf, et al., "Adrenal neoplasms: Effectiveness and safety of CT-guided ablation of 23 tumors in 22 patients," *EJR* , Vol. 81, 1717–1723, 2011.
11. X. Li, et al., "CT-Guided Percutaneous Microwave Ablation of Adrenal Malignant Carcinoma," *Cancer* , Vol. 117, No. 22, 5182–5188, 2011.
12. B. T. McWilliams, et al., "A Directional Interstitial Antenna for Microwave Tissue Ablation: Theoretical and Experimental Investigation," *IEEE Trans Biomed Eng* , Vol. 62, No. 9, 2144–2150, 2015.
13. Y. Mohtashami, et al., "Non-coaxial-based microwave ablation antennas for creating symmetric and asymmetric coagulation zones," *J Appl Phys* , Vol. 123, No. 21, 31–38, 2018.
14. J. Sebek, et al., "Analysis of minimally invasive directional antennas for microwave tissue ablation," *Int J Hyperthermia* , Vol. 33, No. 1, 51–60, 2017.
15. G. Ruvio, et al., "Numerical evaluation of microwave thermal ablation to treat small adrenocortical masses," *Int J RF Microw Comput Eng* , Vol. 28, No. 3, 2018.
16. A. Bottiglieri, et al., "Microwave Thermal Ablation: focusing energy in target tissue using fat layer," in *Proceedings of 13th European Conference on Antennas and Propagation (EUCAP)*, Krakow, Poland, April 2019 [accepted].

17. A. Bottiglieri, et al., "Exploiting tissue boundaries to shape microwave thermal ablation zones," [under submission].
18. A. Shahzad, et al., "Broadband Dielectric Properties of Adrenal Gland for Accurate Anatomical Modelling in Medical Applications," in *Proceedings of 2017 International Conference on Electromagnetics in Advanced Applications (ICEAA)*, Verona, Italy, September 2017.
19. V. Lopresto, et al., "Experimental characterisation of the thermal lesion induced by microwave ablation," *Int J Hyperthermia* , Vol. 30, No. 2, 110–118, 2014.
20. L. Farina, et al., "Characterisation of tissue shrinkage during microwave thermal ablation," *Int J Hyperthermia* , Vol. 30, No. 7, 419–428, 2014.